Article

Structure and Electronic Spectra of DNA Mini-hairpins with G:C Stems

Jennifer Tuma, Stefano Tonzani, George C. Schatz, Andrew H. Karaba, and Frederick D. Lewis

J. Phys. Chem. B, **2007**, 111 (45), 13101-13106• DOI: 10.1021/jp072303m • Publication Date (Web): 25 October 2007

Structure and Electronic Spectra of DNA Mini-hairpins with G_n:C_n Stems

Jennifer Tuma,[†] Stefano Tonzani,[‡] George C. Schatz,[‡] Andrew H. Karaba,[‡] and Frederick D. Lewis*[,‡]

Max Planck Institute for Biophysical Chemistry, Am Fassberg 11, Göttingen, Germany, and Department of Chemistry, Northwestern University, Evanston, Illinois 60208

Received: March 22, 2007; In Final Form: August 19, 2007

The solution structure of a synthetic DNA mini-hairpin possessing a stilbenediether linker and three G:C base pairs has been obtained using ^{1}H NMR spectral data and constrained torsion angle molecular dynamics. Notable features of this structure include a compact hairpin loop having a short stilbene-guanine plane-to-plane distance and approximate B-DNA geometry for the three base pairs. Comparison of the electronic spectra of mini-hairpins having one-to-four G:C base pairs and stilbenediether or hexamethyleneglycol linkers reveals the presence of features in the UV and CD spectra of the stilbene-linked hairpins that are not observed for the ethyleneglycol-linked hairpins. Investigation of the electronic structure of a stilbene-linked hairpin having a single G:C base pair by means of time-dependent density functional theory shows that the highest occupied molecular orbital, but not the lowest unoccupied molecular orbital, is delocalized over the stilbene and adjacent guanine. The calculated UV and CD spectra are highly dependent upon hairpin conformation, but reproduce the major features of the experimental spectra. These results illustrate the utility of an integrated experimental and theoretical approach to understanding the complex electronic spectra of π-stacked chromophores.

Introduction

Hairpin structures consisting of a loop region connecting a base-paired stem are one of the fundamental structural motifs of nucleic acids.[1,2] The structure and stability of DNA and RNA hairpins is dependent upon the base sequence of both the loop and stem regions. Mini-hairpins possessing as few as two canonical Watson−Crick base pairs have been prepared using both trinucleotide and synthetic loops. Hirao and co-workers have investigated the mini-hairpins formed by 5′-d(G:CGAAG:C) and related oligonucleotides and find that they form stable, compact structures having two G:C base pairs.[3,4] We have reported the synthesis and X-ray crystallographic structure of a synthetic hairpin having a stilbenediether (Sd) linker (5′-G(BrU)-TTTG-Sd-CAAAAC), which has a compact loop region and a base paired B-DNA stem.[5,6] Sd-linked mini-hairpins possessing 2−6 A:T base pairs display circular dichroism (CD) spectra characteristic of B-DNA; however the CD spectrum of a Sd-linked hairpin possessing three G:C base pairs is similar to that of G-C rich duplexes that adopt Z-DNA structures.[7]

Our interest in the stepwise evolution of the structure and electronic properties of DNA base pairs[8,9] led us to investigate synthetic mini-hairpins possessing G_n-C_n base paired stems connected by synthetic Sd and hexaethylene glycol (EG) linkers (Chart 1 and 2). We report here the solution structure of the mini-hairpin 5′-CCC-Sd-GGG (Sd-3), as determined by ^{1}H NMR spectroscopy and the UV and CD spectra of both Sd- and EG-linked mini-hairpins. The solution structure of 5′-CCC-Sd-GGG has a compact loop region and a B-DNA stem, in which the base pairs are underwound. The EG-linked hairpins possessing two or more base pairs display CD spectra similar to those of other short poly(G)-poly(C) duplex sequences. However, the Sd-linked poly(G)-poly(C) mini-hairpins display anomalous CD spectra with a strong negative band near 285 nm, which is present even in the case of the conjugate possessing

CHART 1: Structures of Stilbenediether (Sd) and Hexamethylene Glycol (EG) Hairpin Linkers

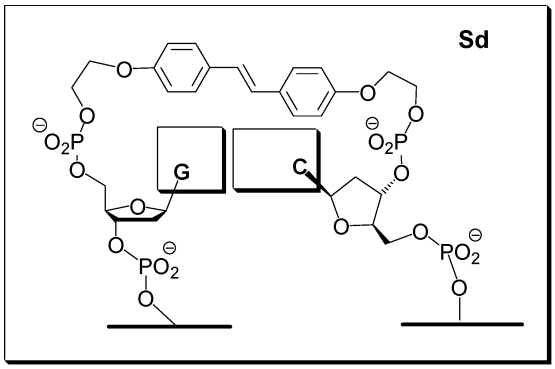

* To whom correspondence should be addressed. E-mail: fdl@northwestern.edu.
[†] Max Planck Institute for Biophysical Chemistry.
[‡] Northwestern University.

10.1021/jp072303m CCC: $37.00
Published on Web 10/25/2007

CHART 2: Structures of Sd- and EG-linked Mini-hairpins

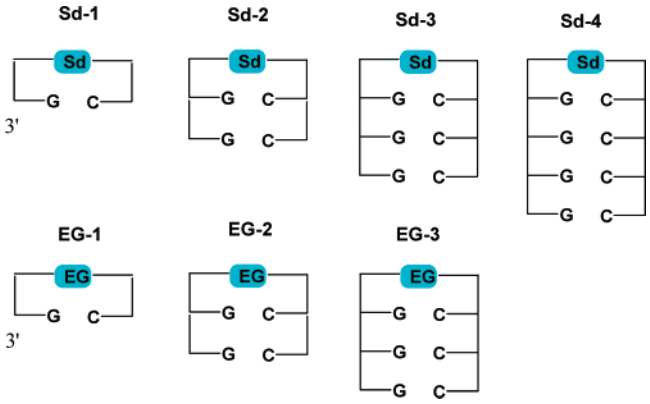

a single G:C base pair. The electronic structure and spectra of the Sd-1 hairpin have been investigated using time-dependent density functional theory(TDDFT). The HOMO of this hairpin is found to be delocalized over the stilbene and adjacent guanine, as previously observed for Sd-linked hairpins with adjacent A-T base pairs by Beljonne et al.[10] The calculated CD spectrum of Sd-1 and, to a lesser extent, its UV spectrum are found to be highly dependent upon molecular conformation. The spectra calculated using structures derived from NMR and molecular dynamics reproduce the major features of the experimental spectra. These results provide the first application of an integrated experimental and theoretical approach to understanding the structure-dependence of the electronic interactions and spectra of simple systems involving DNA-base pairs.

Experimental Section

Materials. The preparation of *trans-N,N′*-bis(3-hydroxylpropyl)stilbene-4,4′-diether and its conversion to the monoprotected, mono-activated diol by sequential reaction with 4,4′-dimethoxytrityl chloride and with 2-cyanoethyl diisopropylchlorophosphoramidite have been elsewhere described.[7] The EG linker was prepared using DMT-protected phosphoramidites purchased from Glen Research (Spacer 18). Hairpin sequences were synthesized by means of conventional phosphoramidite chemistry starting from 3′-phosphate CPG as solid support using a Millipore Expedite DNA synthesizer and following the procedure of Letsinger and Wu.[11] Following synthesis, the conjugates were isolated as trityl-on derivatives by reverse phase (RP)-HPLC, detritylated in 80% acetic acid for 30 min, and repurified by RP-HPLC as needed. RP-HPLC analysis was carried out on a Dionex chromatograph with a Hewlett−Packard Hypersil ODS-5 column (4.6 × 250 mm) and a 1% gradient of acetonitrile in 0.03 M triethylammonium acetate buffer (pH 7.0) with a flow rate of 1.0 mL/min. Molecular weights were determined following desalting by means of MALDI-TOF mass spectroscopy (Table 1).

TABLE 1: MALDI-TOF Data for the Hairpin Conjugates

sequence[a]	calcd mass (g/mol)	observed, *m/z*
EG-1	900.27	899.51
EG-2	1519.11	1517.13
EG-3	2136.46	2134.91
SD-1	918.74	917.17
SD-2	1537.13	1535.79
SD-3	2155.51	2153.76
SD-4	2773.90	2773.41

[a] See Charts 1 and 2 for structures.

UV and CD Spectra. UV spectra were obtained using a Perkin−Elmer Lambda 2 UV spectrophotometer equipped with a Peltier sample holder and a temperature programmer for automatically increasing the temperature at the rate of 0.5 °C/min. Spectra were measured for aqueous solutions of 3−5 μM conjugate in 5 mM lithium phosphate buffer (pH 7.05) in 1 cm path length quartz cells using single scan with a scan speed of 120 nm/min. Circular dichroism spectra were obtained using a JASCO J-715 Spectropolarimeter for aqueous solutions of 3−5 μM conjugate in 5 mM lithium phosphate buffer (pH 7.05) in 1 cm path length quartz cells. Spectra were obtained from the sum of five scans over the 200−400 nm wavelength range with a scan speed of 100 nm/min, a bandwidth of 2.0 nm, and a response time of 2 s. The spectra were corrected by subtraction of a background scan obtained for the buffer solution. UV and CD spectra recorded in 10 mM sodium phosphate buffer (pH 7.2) with 150 mM NaCl were identical to those recorded in lithium phosphate buffer.

NMR Spectra and Structure Generation. Samples of 5′-CCC-Sd-GGG used for NMR experiments were first lyophilized four times from aqueous NH_4OH solution (10%) to remove residual triethylamine and then twice from D_2O. The samples were dissolved in 200 μL either in D_2O (99.999% D), or H_2O/D_2O (9:1), containing 150 mM NaCl and 10 mM phosphate buffer (pH 7, uncorrected for deuterium effect) and then transferred to NMR microtubes (Shigemi Co., Tokyo, Japan). The final concentration of the DNA-hairpin was 1 mM.

Distance restraints were derived by integration of NOESY cross-peaks of the spectrum at a mixing time of 300 ms. The intensities were calibrated on known distances, such as the H5 and H6 of cytosine and divided in classes of strong (2.5 Å), medium (3.0 Å) and weak (3.5−4.5 Å). The distances were entered as constraints with boundaries of ±0.5 or 1.0, depending on the quality of the cross-peak. Isochronous protons of the stilbene were treated with pseudoatom approach, using the averaging function "sum", rather than the geometric center pseudoatom approach, employed for diastereotopic protons from the deoxyribose residues.

The imino proton signals observed in spectra acquired in H_2O/D_2O showed the characteristic chemical shifts of protons engaged in hydrogen bonding within Watson−Crick base pairs. Thus, base pairing constraints (hydrogen bonding and base pair planarity) were introduced in the molecular dynamics calculations, using the default values of the program CNS.[12] The NOESY cross-peaks between protons of neighboring nucleotides are those expected for an undisrupted B-form duplex. Further, all the ^3J (H1′/H2′) coupling constants, derived by P.E.COSY, have values of 8 ± 1 Hz, typical for the 2′-endo conformation.[13] On the basis of this information, constraints for the backbone dihedral angles were entered for B-form DNA, as described in the literature (boundaries of ±20°).[14]

Topology and parameter files for the molecular dynamics calculation were generated using the X-PLOR files for DNA,[15] modified for the stilbene residue. The additional values for the stilbene-bridge were derived by an X-ray crystal structure[6] and implemented with the help of XPLO2D.[16] The two covalent bonds from the stilbene residue to the terminal C-G-base pair were created using the X-PLOR input file "generate.inp". Restrained molecular dynamics calculations were performed in CNS version 1.0 with the torsion angle molecular dynamic protocol.[17] Statistical data for the lowest energy structures are summarized in Table 2. The structures were improved by visualizing and detecting the restraints in VMD-X-PLOR[18] and via back-calculated NOESY spectra, generated in GIFA.[19]

TABLE 2: Statistical Data on the Structure of Sd-3 as Determined by Restrained Molecular Dynamics

constraints		lowest energy structures (15)	
NOE-based total	36	NOE constraint violation	0 (<0.5 Å)
interresidue	7	dihedral angle constraints violation	0 (<30°)
intraresidue	12	rmsd from average (all coordinates)	0.88 Å
DNA-STI	17	pairwise rmsd (all coordinates)	1.30
dihedral angle constraints	21	energy, kcal/mol	-203 ± 6
hydrogen bond constraints	12		
base pair planarity constraints	3		

Isochronous protons of the stilbene moiety appear at the same chemical shift. Therefore these constraints for the structure calculation were used as ambiguous in the structure calculations.

Calculations. In order to calculate the absorption and CD spectra of the hairpin with only one G:C base pair (**Sd-1**), we have performed molecular dynamics simulations at 300 K similar to those described previously,[9] using the Amber 8 package.[20] Simulations were run for 2.0 ns after minimizing structures generated from ideal B-DNA parameters. During the final 1.5 ns, the root-mean-squared-deviation (RMSd) from the averaged structure obtained during the first 0.5 ns was monitored to ensure that the system had reached equilibrium. Snapshots taken at least 5 ps apart were used to calculate UV and CD spectra using the ADF density functional package.[21−23]

Time-dependent density functional theory (TDDFT) calculations were performed using a triple-ζ plus polarization (TZP) Slater basis set, and the XC functional employed was SAOP,[24] which is an asymptotically correct functional and, as such, will yield correct excitation energies for states that have substantial Rydberg character. This is important because of the need to converge a large number of excited states. Spurious low-energy charge transfer states do not seem to constitute a problem due to the small size of the system and the fact that $\pi-\pi$ stacking guarantees orbital overlap between stilbene and base pair. The DFT calculations were performed neglecting the backbone structure and filling the valences with hydrogen atoms, since the backbone is expected to absorb below 180 nm and not in the low-energy spectral region in which we are interested. Solvation is expected to shift the spectral peaks slightly[25] and thus was not included. As a test of this assumption, spectra for stilbene were calculated using a continuum solvation model (COSMO)[26] and the solvent shifts were found to be on the order of 0.1 eV. Due to error compensation in the DFT calculations, the energy of peaks in the base pair region is very close to the experimental results without the inclusion of solvation.

Results and Discussion

Solution Structure of Hairpin Sd-3. The sequence 5′-CCC-Sd-GGG (Chart 2, **Sd-3**) has previously been reported to form a stable base-paired hairpin structure having a melting temperature > 80 °C, as determined from the 260 nm thermal dissociation profile.[7] One- and two-dimensional NMR spectra are consistent with the presence of a single major conformation. Two conformers only differing in the position of the ethylene unit (flipped by 180°) were derived. The 15 lowest energy violation-free structures obtained from restrained molecular dynamics calculations are shown in Figure 1. The averaged structure of **Sd-3**, as viewed from the side and perpendicular to the Sd molecular plane, is shown in Figure 2. The hairpin loop is compact, having an average stilbene-to-G:C plane-to-plane distance of 3.0 ± 0.2 Å. This value is shorter than the 3.25 ± 0.1 Å plane-to-plane distance in Egli's crystal structure for G(BrU)TTTG-Sd-CAAAAC[6] and significantly shorter than the average 3.4 Å distance between base pairs in B-DNA.[1]

The view perpendicular to the stilbene plane (Figure 2b) shows a sandwich-like geometry for stilbene and guanine, but little overlap with cytosine. The linkages formed by the two flexible ethylene diether connectors are also different, the extended linkage to the 5′-guanine having an anti conformation and the compact linkage to the 3′-cytosine having a gauche conformation. Both of the ethylene units in Egli's crystal structures adopt gauche confomations, as is typical for poly-(ethylene oxides).[6] The stem region of **Sd-3** adopts a right-hand helical geometry with "normal" B-DNA stacking distances between adjacent base pairs. However, the average twist angle is ~41°, somewhat larger than the average value of 36° for B-DNA. It is possible that torsional strain in the compact loop structure results in overwinding of the base pair stem.

The π-stacking interaction between the stilbene and adjacent G:C base pair in **Sd-3** is similar to that of a trimethoxystilbene modified DNA duplex in which the stilbene moiety is 5′-tethered to the 5′-terminal thymine of a self-complementary oligonucleotide.[27] This duplex adopts two conformations related by a 180° flip of the stilbene which differ in the orientation of the stilbene ring system relative to the adjacent A:T base pair. By contrast, the position of the stilbene is invariant in the 15 lowest energy structures of **Sd-3**. The average twist angle for the end-capped duplex is 39°, intermediate between that for **Sd-3** and 36°.

Ultraviolet Spectra. The ultraviolet spectra of the mini-hairpins are shown in Figure 3. The spectra of the Sd-linked hairpins display a long-wavelength absorption band at 327 nm assigned to the stilbene π,π^* transition and a shorter wavelength band assigned to the overlapping absorption of the stilbene and nucleobases.[7] Only the shorter wavelength band is present in the spectra of the EG-linked hairpins. The shape of the 260 nm band is dependent upon the number of bases in the conjugate structure, the 275 nm shoulder which is clearly resolved in the spectrum of guanine becoming weaker as the number of bases increases. The 260 nm UV intensities of the Sd- and EG-linked

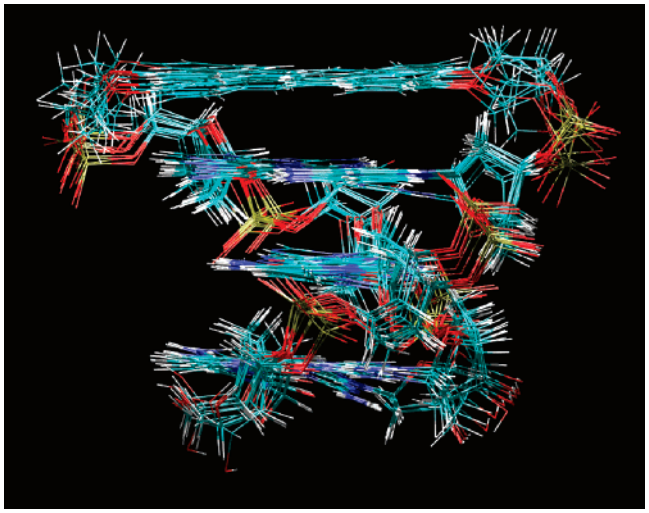

Figure 1. Overlay of the 15 lowest energy, violation-free structures for **Sd-3**, as obtained from restrained molecular dynamics calculation.

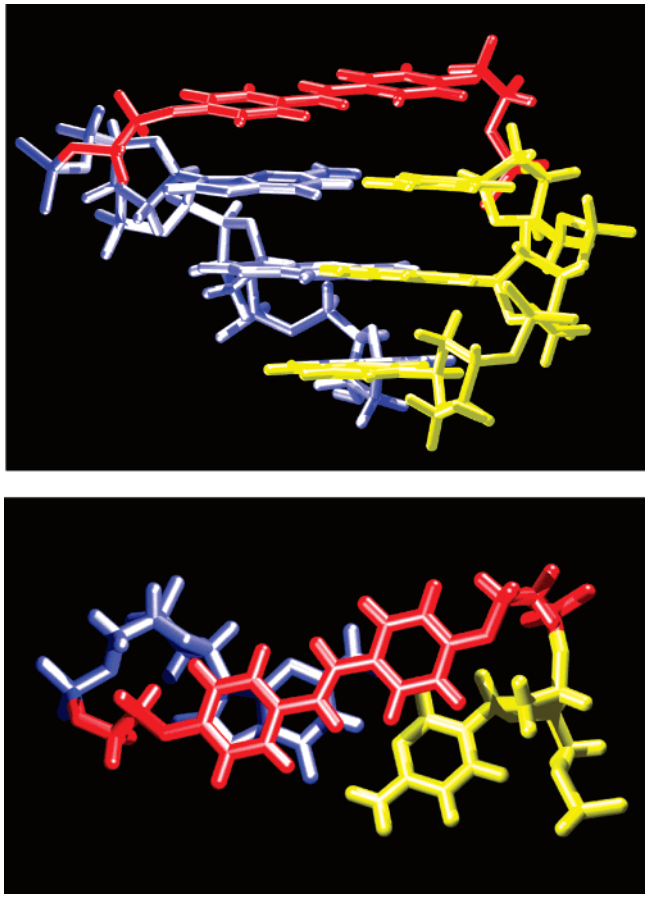

Figure 2. Lowest energy structure of **Sd-3** as viewed from the side and the hairpin loop region as viewed from above (only one base pair shown), with the Sd linker shown in red, guanine in blue, and cytosine in yellow.

conjugates change only slightly upon heating from 5 to 90 °C, as previously reported for **Sd-3**.[7]

Quantum chemical calculations of the electronic coupling between the Sd hairpin linker and an adjacent A-T base pair have previously been reported by Beljonne et al.[10] In accord with their description of the highest filled orbitals, we find partial delocalization of the HOMO **Sd-1** on guanine (Figure 4) and of the HOMO-1 on stilbene (the LUMO is localized on stilbene), assuming a structure for **Sd-1** based on the NMR derived structure for the linker and adjacent G-C base pair of **Sd-3**. There is a lesser degree of delocalization and more pronounced dependence on the structural parameters in our calculations for **Sd-1** than in the calculations of Beljonne et al.[10] The calculated absorption spectra of **Sd-1** obtained using the NMR-derived structure for the linker and first G:C base pair and for an average of 28 snapshots obtained from the last 1.5 ns of the molecular dynamics simulations of the structure are shown in Figure 5. The calculated spectra underestimate the absorption frequency of the Sd linker, resulting in a red shift of its spectrum by roughly 0.4 eV, compared to the experimental result (Figure 3). We attribute this partially to the fact that we are using a pure density functional, but also to the tendency of DFT to "overdelocalize" electrons in an extended conjugated system. The description of the Sd absorption is somewhat worse than that of the base pairs, whose absorption spectra are relatively well represented by DFT.[28]

Circular Dichroism Spectra. The CD spectra of the Sd- and EG-linked hairpins are shown in Figure 6. The spectral band shapes of **EG-2** and **EG-3** are similar in appearance to those reported for the self-complementary poly[d(G_2C_2)] and poly-

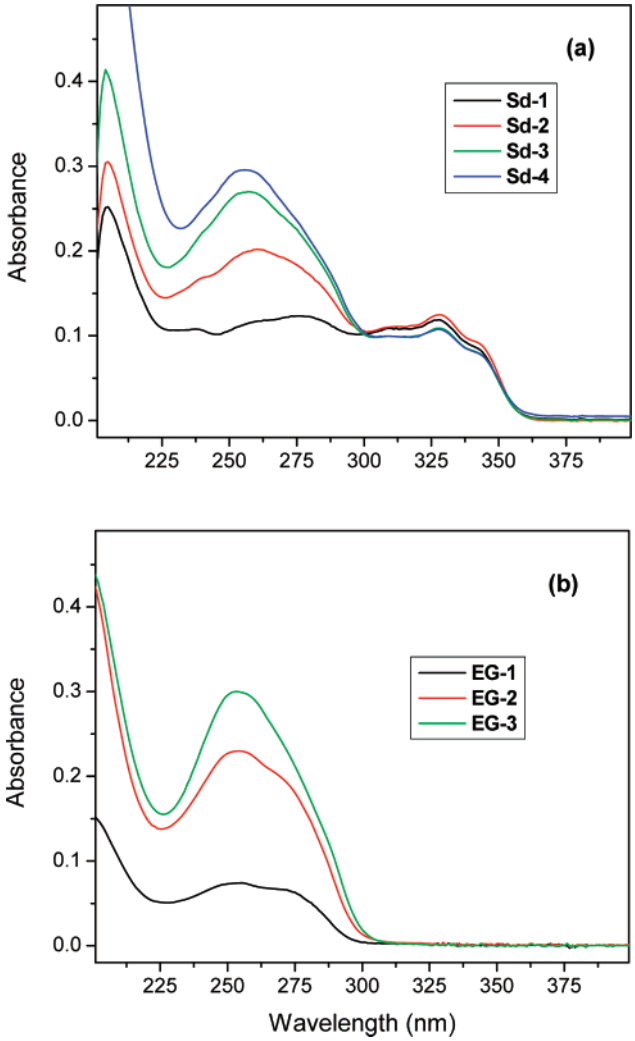

Figure 3. UV spectra of mini-hairpins (a) **Sd-1**−**4** (3 μM) and (b) **EG1**−**3** (5 μM) in aqueous solution containing 5 mM lithium phosphate (pH 7.05).

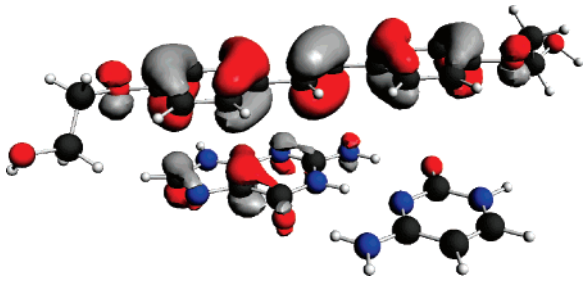

Figure 4. HOMO orbital (in gray and red) for **Sd-1** delocalized on the stilbene (top) and partially on the guanine (bottom left) from DFT calculations using the NMR-derived structure for **Sd-3**.

[d(G_3C_3)], respectively, when corrected for the contributions of [d(G:C)] steps.[29] As a test of our computational methodology, we have calculated the CD spectrum for two G:C base pairs having an ideal B-DNA geometry. The results shown in Figure 7 are in good agreement with the experimental spectra of **EG-2** and **EG-3**. Since the calculated spectra are sensitive to conformation, this suggests that the EG-linked hairpins have conformations very close to that of B-DNA and that conformational fluctuations average to zero.

The CD spectra of hairpins **Sd-1**−**4** (Figure 6a) are anomalous in that they display a negative band between 280 and 284 nm, a region for which poly[d(G_nC_n)] duplexes and the hairpins **EG-2,3** display weak positive bands (Figure 6b). Furthermore, a

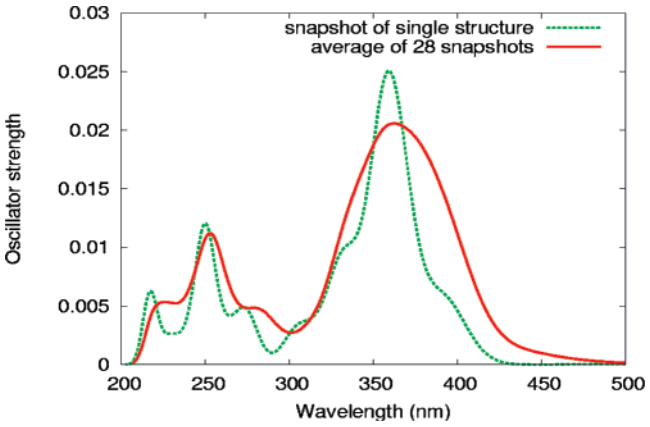

Figure 5. UV spectra calculated for the **Sd-1** hairpin using a single structure derived from the NMR structure of **Sd-3** and from the average of 28 snapshots.

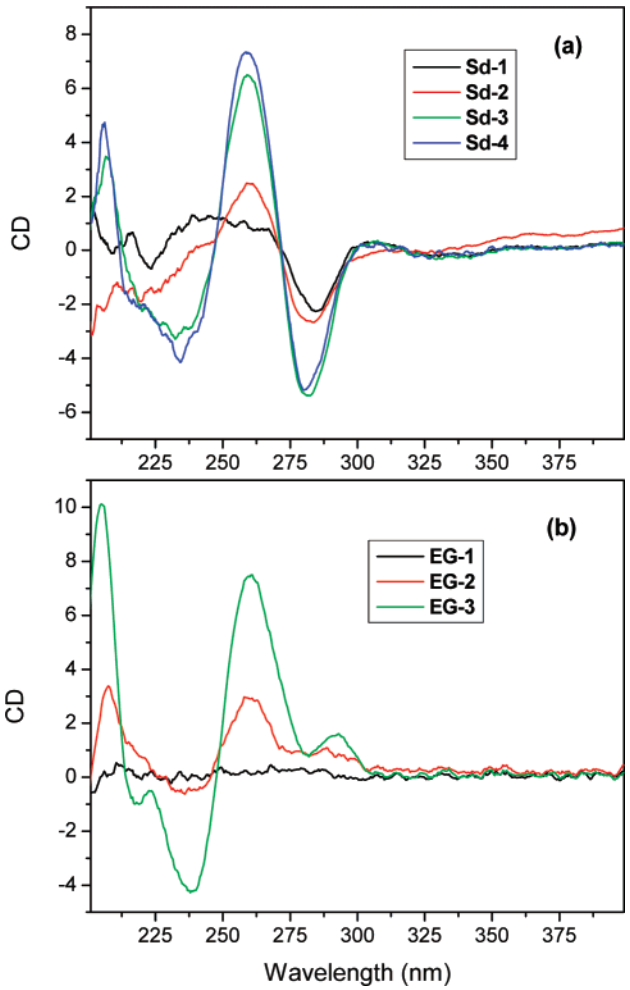

Figure 6. CD spectra of mini-hairpins (a) **Sd-1**−**4** (3 μM) and (b) **EG1**−**3** (5 μM) in aqueous solution containing 5 mM lithium phosphate (pH 7.05).

negative 284 nm band is observed even in the case of **Sd-1**, which possesses a single G:C base pair. However, this band is not present in the conjugate 5′ G-Sd-C which has reversed polarity or in 5′ Sd-G or 5′ Sd-C which lack a base pair.[19] As the number of G:C base pairs increases, the intensity of this band increases, as does that of the positive 260 nm band, which is similar in band shape and intensity to that of the **EG-2,3** hairpins. Negative bands in the 280−300 nm region have been observed for Z-form poly[d(G_nC_n)] at high salt concentration.[30]

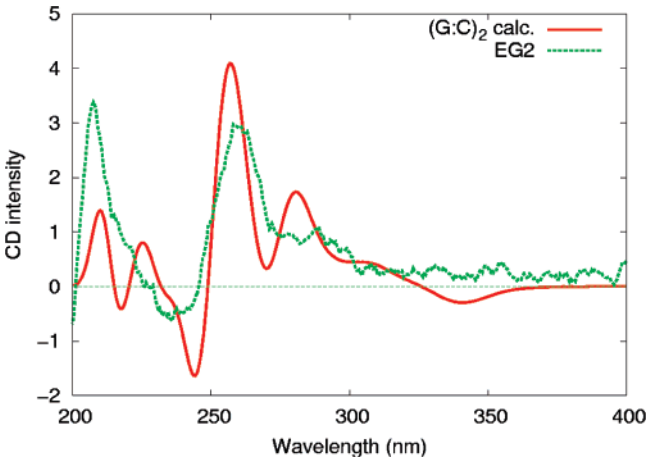

Figure 7. CD spectrum calculated for two adjacent GC base pairs stacked as in the ideal B-DNA geometry and the experimental spectrum for **EG-2**.

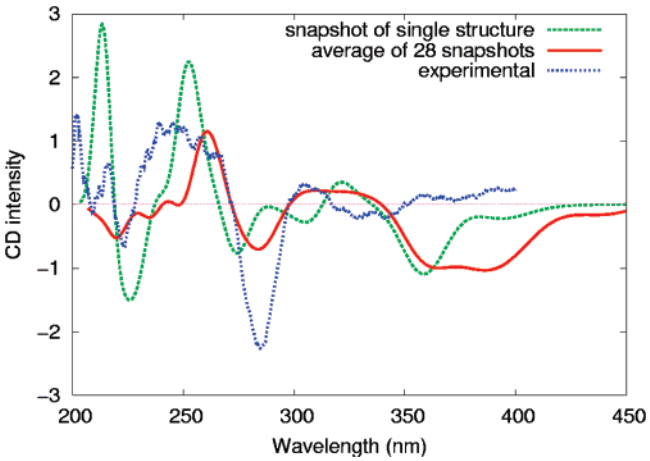

Figure 8. CD spectra calculated for the **Sd-1** hairpin using a single structure derived from the NMR structure of **Sd-3** and from the average of 28 snapshots. The experimental spectrum of **Sd-1** is shown for purposes of comparison.

However, the ^{1}H NMR spectra of **Sd-3** clearly establish that it adopts a B-form structure in dilute solution.

We have calculated the CD spectra of **Sd-1** both for a single geometry obtained from the NMR-derived structure and for the average of 28 snapshots derived from the last 1.5 ns of the MD simulations. As seen in Figure 8, the calculated CD spectra correctly reproduce the main features seen in the experimental spectrum of **Sd-1**, namely the negative peak at 280 nm and positive peaks at 310 and 260 nm, although the agreement is not perfect due to the flexible nature of the system. Better agreement of calculated and experimental spectra in the high-energy region (200−320 nm) is obtained by averaging over multiple snapshots. The level of averaging was found to be important, as there is considerable variation in the CD spectra with structure. In the low-energy region (320−400 nm), where the oscillator strength of the stilbene is concentrated, many strong peaks of opposite signs tend to cancel each other, so it is difficult to converge the average over configurations. It appears that further averaging will lead to better agreement with experiment, but since this region of the experimental spectra is not particularly interesting, we did not pursue this further.

Concluding Remarks

Previous studies of mini-hairpins with non-nucleotide linkers have employed either mix-base stems or poly(A)-poly(T)

stems.[11,31,32] The present study establishes for the first time the formation of stable Sd- and EG-linked mini-hairpins having short G:C base paired stems. The absence of distinct melting transitions prevents direct comparison of the stability of Sd- vs EG-linked hairpins. However, we have found that Sd-linked hairpins having poly(A)-poly(T) stems are more stable than their EG-linked analogs.[33]

The structure derived from NMR and molecular dynamics calculations for **Sd-3** establishes that it adopts a hairpin structure with a B-DNA stem, rather than forming a duplex between two self-complementary 5′-d(CCC-Sd-GGG) conjugates. A duplex structure would be expected to display strong exciton-coupled CD bands for the adjacent stilbene chromophores, which is not observed for **Sd-3**.[9] A similar preference for hairpin vs duplex structures has been observed for Sd-linked hairpins having poly-(A)-poly(T) stems.[7] The exceptional stability of the Sd-linked mini-hairpins is most likely a consequence of their highly compact loop regions. The distance between the Sd linker and proximate G:C base pair in **Sd-3** is 3.0 ± 0.2 Å, substantially shorter than the average 3.4 Å rise for B-DNA.[1]

The short stacking distance and extensive overlap between the Sd and guanine π-surfaces are also responsible for the anomalous CD spectra of the Sd-linked hairpins **Sd-1**−**4**. We have employed density functional theory to investigate the electronic interactions in hairpin **Sd-1** and its absorption and CD spectra. These calculations accurately reproduce the main features of the spectra, although the intensity of some peaks tends to be too large. Averaging over multiple conformations may be necessary in order to obtain better agreement of experimental and calculated spectra. It is interesting to note that the calculated CD spectrum obtained using B-DNA parameters for this hairpin provides a poor match for the experimental spectrum. This suggests that structural details are very important.

The TDDFT calculations also establish that exciton coupling between nucleobases and adjacent chromophores can have a significant impact on the appearance of the UV and CD spectra. This is an encouraging result, suggesting that TDDFT calculations may be applied to larger systems, provided that an averaged or lowest energy structure is available. Exciton coupling interactions between chromophores and base pairs were neglected in our earlier studies of exciton coupling interactions between stilbenediamide chromophores in capped hairpin and dumbbell structures.[9,34] The CD spectra of these systems in the long-wavelength region (300−400 nm) are described well by an analytic model in which B-DNA structural parameters were used.[9] In that case, the chromophores were separated by base pairs, and their coupling was probably less sensitive to the detailed variation of all the structural parameters.

Acknowledgment. Financial support for this research was provided by grants from the National Science Foundation (CHE-0628130 to FDL and GCS), DURINT (to GCS), and the European Commission (NMP4-CT-2003-505669 to JT). The Northwestern authors thank Huihe Zhu, Ligang Zhang, Xiaobing Zuo, Lasse Jensen, Martin McCullagh, and Ferdinand C. Grozema for assistance and advice. ST thanks PNNL for supercomputing time. JT thanks Prof. C. Richert for helpful discussions and Prof. C. Griesinger for generous support and providing access to NMR resources.

Supporting Information Available: Figure S1, showing an overlay of experimental (red) and back-calculated (black) NOESY spectra of **Sd-3**, and Figure S2, showing the CD spectra of several reference conjugates. This material is available free of charge via the internet at http://pubs.acs.org.

References and Notes

(1) Bloomfield, V. A.; Crothers, D. M.; Tinoco, I., Jr. *Nucleic Acids, Structures, Properties, Functions*; University Science Books: Sausalito, 2000.

(2) Neidle, S. *Oxford Handbook of Nucleic Acid Structure*; Oxford University Press: Oxford, 1999.

(3) Hirao, I.; Kawai, G.; Yoshizawa, S.; Nishimura, Y.; Ishido, Y.; Watanabe, K.; Miura, K. *Nucleic Acids Res.* **1994**, *22*, 576−582.

(4) Yoshizawa, S.; Kawai, G.; Watanabe, K.; Miura, K.; Hirao, I. *Biochemistry* **1997**, *36*, 4761−4767.

(5) Egli, M.; Tereshko, V.; Mushudov, R.; Sanishvili, R.; Liu, X.; Lewis, F. D. *J. Am. Chem. Soc.* **2003**, *125*, 10842−10849.

(6) Lewis, F. D.; Liu, X.; Wu, Y.; Miller, S. E.; Wasielewski, M. R.; Letsinger, R. L.; Sanishvili, R.; Joachimiak, A.; Tereshko, V.; Egli, M. *J. Am. Chem. Soc.* **1999**, *121*, 9905−9906.

(7) Lewis, F. D.; Wu, Y.; Liu, X. *J. Am. Chem. Soc.* **2002**, *124*, 12165−12173.

(8) Lewis, F. D.; Liu, X.; Wu, Y.; Zuo, X. *J. Am. Chem. Soc.* **2003**, *125*, 12729−12731.

(9) Lewis, F. D.; Zhang, L.; Liu, X.; Zuo, X.; Tiede, D. M.; Long, H.; Schatz, G. S. *J. Am. Chem. Soc.* **2005**, *127*, 14445−14453.

(10) Beljonne, D.; Pourtois, G.; Ratner, M. A.; Bredas, J. L. *J. Am. Chem. Soc.* **2003**, *125*, 14510−14517.

(11) Letsinger, R. L.; Wu, T. *J. Am. Chem. Soc.* **1995**, *117*, 7323−7328.

(12) Brünger, A. T.; Adams, P. D.; Clore, G. M.; DeLano, W. L.; Gros, P.; Grosse-Kunstleve, R. W.; Jiang, J.-S.; Kuszewski, J.; Nilges, N.; Pannu, N. S.; Read, R. J.; Rice, L. M.; Simonson, T.; Warren, G. L. *Acta Crystallogr.* **1988**, *D54*, 905−921.

(13) Wijmenga, S.; Mooren, M.; Hilbers, C. In *NMR of Macromolecules: A Practical Approach*, Roberts, G. C. K., Ed.; Oxford University Press: Oxford (UK), 1993.

(14) Saenger, W. *Principles of Nucleic Acid Structure*; Springer: New York, 1984.

(15) Brünger, A. *X-PLOR, version 3.1 X-PLOR Manual*, Yale Universtiy Press: New Haven, 1992.

(16) Kleywegt, G. J.; Jones, T. A. *Acta. Cryst.* **1988**, *D54*, 1119−1131.

(17) Stein, E. G.; Rice, L. M.; Brunger, A. T. *J. Magn. Reson. Ser. B* **1997**, *124*, 154−164.

(18) Schwieters, C. D.; Clore, G. M. *J. Magn. Reson.* **2001**, *149*, 239−244.

(19) See Supporting Information.

(20) Cornell, W. D.; Cieplak, P.; Bayly, C. I.; Gould, I. R.; Merz, K. M.; Ferguson, D. M.; Spellmeyer, D. C.; Fox, T.; Caldwell, J. W.; Kollman, P. A. *J. Am. Chem. Soc.* **1996**, *118*, 2309−2309.

(21) Baerends, E. J.; Autschbach, J.; Berces, A. *ADF*, Vrije Universiteit, Amsterdam, The Netherlands, 2005, http://www.scm.com.

(22) te Velde, G.; Bickelhaupt, F. M.; Baerends, E. J.; Fonseca Guerra, C.; van Gisbergen, S. J. A.; Snijders, J. G.; Ziegler, T. *J. Comput. Chem.* **2001**, *22*, 931−967.

(23) Autschbach, J.; Ziegler, T.; Gisbergen, S. J. A. v.; Baerends, E. J. *J. Chem. Phys.* **2002**, *116*, 6930−6940.

(24) Gritsenko, O. V.; Schipper, P. R. T.; Baerends, E. J. *Int. J. Quantum Chem.* **2000**, *76*, 407−419.

(25) Mennucci, B.; Tonniolo, A.; Tommasi, J. *J. Phys. Chem. A* **2001**, *105*, 4749−4757.

(26) Pye, C. C.; Ziegler, T. *Theor. Chim. Acta* **1999**, *101*, 396−408.

(27) Tuma, J.; Paulini, R.; Rojas Stutz, J. A.; Richert, C. *Biochem.* **2004**, *43*, 15680−15687.

(28) Varsano, D.; Di Felice, R.; Marques, M. A. L.; Rubio, A. *J. Phys. Chem. B* **2006**, *110*, 7129−7138.

(29) Gudibande, S. R.; Jayasena, S. D.; Behe, M. J. *Biopolymers* **1988**, *27*, 1905−1915.

(30) Uesugi, S.; Ohkubo, M.; Ohtsuka, E.; Ikehara, M.; Kobayashi, Y.; Kyogoku, Y. *Nucleic Acids Res.* **1984**, *12*, 7793−7810.

(31) Durand, M.; Chevrie, K.; Chassignol, M.; Thuong, N. T.; Maurizot, J. C. *Nucleic Acids Res.* **1990**, *18*, 6353−6359.

(32) Rumney, S.; Kool, E. T. *J. Am. Chem. Soc.* **1995**, *117*, 5635−5646.

(33) Zhu, H., unpublished results.

(34) Zhang, L.; Long, H.; Schatz, G. C.; Lewis, F. D. *Org. Biomol. Chem.* **2007**, *5*, 450−456.